

Evaluating Image Caption via Cycle-consistent Text-to-Image Generation

Tianyu Cui^{1*} Jinbin Bai² Guo-Hua Wang² Qing-Guo Chen² Zhao Xu²
 Weihua Luo² Kaifu Zhang² Ye Shi^{1†}

¹ ShanghaiTech University ² AI Business, Alibaba Group

{cuity2022, shiye}@shanghaitech.edu.cn

{baijinbin.bjb, wangguohua, qingguo.cqg, changgong.xz, weihua.luowh, kaifu.zkf}@alibaba-inc.com

Abstract

Evaluating image captions typically relies on reference captions, which are costly to obtain and exhibit significant diversity and subjectivity. While reference-free evaluation metrics have been proposed, most focus on cross-modal evaluation between captions and images. Recent research has revealed that the modality gap generally exists in the representation of contrastive learning-based multi-modal systems, undermining the reliability of cross-modality metrics like CLIPScore. In this paper, we propose CAMScore, a cyclic reference-free automatic evaluation metric for image captioning models. To circumvent the aforementioned modality gap, CAMScore utilizes a text-to-image model to generate images from captions and subsequently evaluates these generated images against the original images. Furthermore, to provide fine-grained information for a more comprehensive evaluation, we design a three-level evaluation framework for CAMScore that encompasses pixel-level, semantic-level, and objective-level perspectives. Extensive experiment results across multiple benchmark datasets show that CAMScore achieves a superior correlation with human judgments compared to existing reference-based and reference-free metrics, demonstrating the effectiveness of the framework.

1. Introduction

High-quality image captions are vital for training a product-level vision foundation model. As a task to generate descriptive textual captions for given images, image captioning has garnered substantial attention from the research community in recent years [3, 5, 12, 16, 40]. Furthermore, establishing an automatic evaluation metric that closely aligns with human judgment is crucial for advancing image captioning models effectively. Previous research [13] has

*Work done during the internship at AI Business, Alibaba Group.

†Corresponding author, email: shiye@shanghaitech.edu.cn.

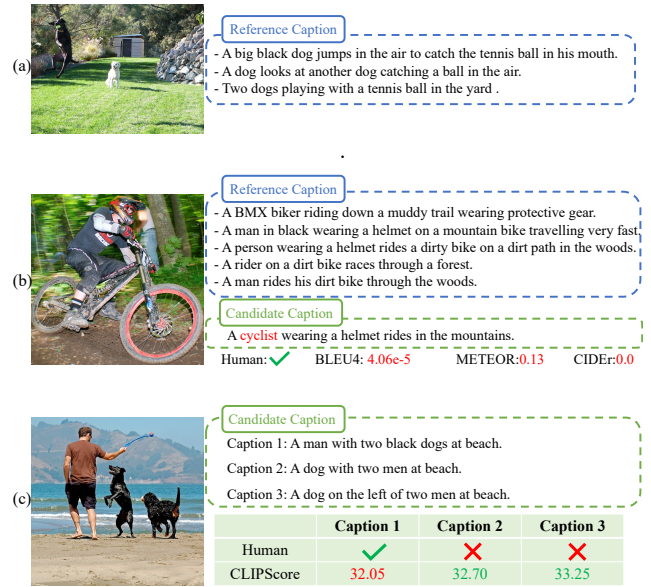


Figure 1. (a) References fail to capture all information in the image, such as the color and position of the white dog. (b) Caption aligns with human judgment, but scores low on reference-based metrics. This discrepancy arises because different caption styles can lead to misalignment between reference-based metric scores and human judgments. (c) Modality gap in cross-modality evaluation can lead to confusion of attributes including numeracy and spatial relationships.

demonstrated that reference-only evaluation metrics correlate poorly with human judgments. As Figure 1 (a) shows, references alone often fail to fully capture the content of an image, leading to less reliability of reference-only evaluation image captioning metrics. Consequently, several approaches [18, 23, 39] have been proposed to integrate both references and images in the evaluation of image captions.

However, the diversity and subjectivity of reference captions pose significant challenges for evaluating image captioning performance [24]. Additionally, collecting ref-

reference captions can be resource-intensive, and even the availability of multiple human-authored captions per image often proves insufficient for comprehensive assessment [13, 24]. As illustrated in Figure 1 (b), various caption styles can lead to misalignment between reference-based metric scores and human judgments.

To address these limitations, reference-free evaluation metrics have been proposed, which directly utilize images instead of reference captions in the evaluation process. Nonetheless, previous reference-free evaluation metrics predominantly focus on cross-modality evaluation between captions and images. Recent studies [26, 35] have revealed that the modality gap generally exists in the representation of contrastive learning-based multi-modal systems, undermining the reliability of cross-modality evaluation metrics like CLIPScore [13]. As shown in Figure 1 (c), CLIPScore, which relies solely on overall similarity, lacks fine-grained evaluation capabilities and may confuse attributes including numeracy and spatial relationships.

In this paper, we proposed CAMScore, a cyclic reference-free automatic evaluation metric for image captioning models. To circumvent the aforementioned modality gap, CAMScore utilizes a text-to-image model to generate images from captions and subsequently evaluates these generated images against the original images. By performing evaluations within the same image modality, CAMScore enables reference-free evaluation while addressing the modality gap inherent in existing cross-modality metrics, which exploits the cycle consistency across modalities.

Furthermore, to provide fine-grained information for a more comprehensive evaluation, we design a three-level evaluation framework for CAMScore. Specifically, this modular framework encompasses pixel-level, semantic-level, and objective-level evaluations, offering comprehensive evaluation from three distinct perspectives and thereby enhancing the robustness and accuracy of the metric.

To verify the effectiveness of CAMScore, we conduct extensive experiments across multiple image captioning benchmarks, aiming to assess the consistency of the proposed metric with human judgments. Specifically, we calculate the Kendall correlation coefficient on Flickr8k-Expert [14], Flickr8k-CF [14] and COMPOSITE [1] datasets, and evaluate the pairwise ranking accuracy on PASCAL-50S [36] dataset. Our experimental results demonstrate that CAMScore achieves a superior correlation with human judgments compared to existing reference-based and reference-free metrics.

In summary, the main contributions of this paper are three-fold:

- We proposed CAMScore, a novel cyclic reference-free evaluation metric for image captioning. By leveraging cycle consistency, CAMScore enables reference-free evaluation while addressing the modality gap inherent in exist-

ing cross-modality metrics, thereby facilitating evaluation within the same image modality.

- We designed a three-level evaluation framework, which provides a modular framework for fine-grained evaluation of image captions from the pixel level, semantic level, and object level perspectives.
- Extensive experiments demonstrate that CAMScore achieves strong correlation with human judgments across various benchmarks including Flickr8k-Expert [14], Flickr8k-CF [14], COMPOSITE [1] and PASCAL-50S [36] datasets, showing the effectiveness of the proposed metric.

2. Related Work

2.1. Image captioning evaluation metrics

According to whether involving image and reference caption, image captioning evaluation metrics can be roughly divided into three categories: reference-only evaluation metrics, reference + image evaluation metrics, and reference-free evaluation metrics.

Reference-only evaluation metrics. This kind of metric [2, 6, 8, 27, 31, 36, 42, 44, 45] focus solely on comparing the reference caption with the candidate caption, primarily relying on n -grams or scene graphs. BLEU [31] calculates the precision between candidate and reference captions, ROUGE [27] measures the recall of the longest common subsequence, and METEOR [6] computes a version of alignment on unigram-level. CIDEr [36] employs tf-idf weighting for each n -gram, SPICE [2] compares semantic propositional content using the predicted scene graph. BERTSCORE [44] and its improved version [42] leverages learned embeddings from a pre-trained language model BERT [8] to represent and measure semantic similarities.

Reference + image evaluation metrics. References alone cannot fully capture the content of an image, making reference-only evaluation metrics for image captioning less reliable. To address this limitation, some approaches [18, 23, 39] integrate both reference captions and images to evaluate image captions. TIGEr [18] utilizing text-to-image grounding results based on a pre-trained SCAN model. ViLBERTScore [23] generates image-conditioned embeddings for each token in candidate and reference captions using ViLBERT [29]. MID [20] uses CLIP visual-textual features to compute negative Gaussian cross-mutual information, resulting in a more effective evaluation metric.

Reference-free evaluation metrics. In the reference + image evaluation metrics, although the image supplements the reference for evaluation, these methods remain inapplicable in the absence of reference. Therefore, reference-free

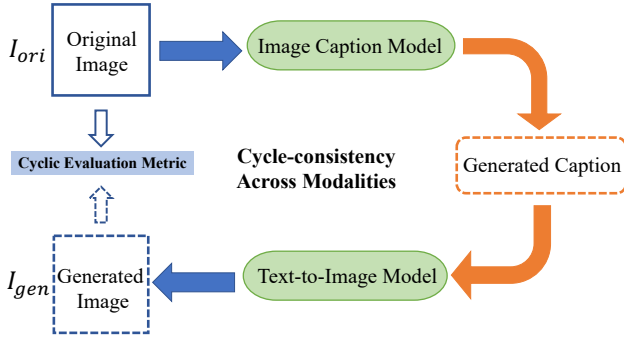


Figure 2. Overview of our proposed framework.

metrics [13, 17, 24, 25] have been proposed to evaluate candidate captions without references. UMIC [24] fine-tunes a pre-trained UNITER [7] via contrastive learning to compute the score of the caption. CLIPScore [13] relies on the image-text similarity from the CLIP model [32]. Based on CLIPScore, PAC-S[33] further fine-tunes CLIP with positive-augmented contrastive learning and evaluates captions in the same manner as CLIPScore. In addition to metrics based on CLIP, there are also methods based on the large multimodal model (LMM). FLEUR [25] leverages LMM to introduce explainability into image captioning evaluation. Previous methods predominantly focus on cross-modality evaluation between captions and images, thereby failing to address the inherent modality gap. Different from previous approaches, we proposed a novel cyclic evaluation metric, CAMScore, which leverages cycle consistency to perform evaluations within the same image modality, thereby circumventing the modality gap.

2.2. Cycle consistency

Our work is influenced by cycle consistency, a method to bridge one modality or domain to the other. Cycle consistency has been widely applied across various tasks, including unpaired image-to-image translation [15, 47], depth estimation [10], visual object tracking [38], visual question answering [34], video-text retrieval [4] and image captioning [11]. Unlike previous approaches that focus primarily on consistency within a single modality or task, our approach jointly forms a cyclic relationship between two modalities (text and image), and two tasks (image captioning and text-to-image task). To the best of our knowledge, cycle consistency between these two tasks has been rarely addressed in the literature. In this work, we leverage cycle consistency for image captioning evaluation, enabling the evaluation reference-free and circumventing the modality gap in existing cross-modality evaluation metrics.

3. Cycle-consistent Evaluation Framework

In this section, we delve into the details of our proposed cycle-consistent evaluation framework. As illustrated in Figure 2, CAMScore evaluates image caption models by employing a frozen text-to-image model to generate images I_{gen} from the caption. These generated images are then compared against the original image I_{ori} across three distinct perspectives. By performing evaluations within the same image modality, CAMScore enables reference-free evaluation while addressing the modality gap inherent in existing cross-modality metrics, which exploits the cycle consistency across modalities.

3.1. Image caption generation module

For a given image, the image captioning model generates a descriptive text caption T_{gen} . The process can be formulated as follows:

$$T_{gen} = G(I_{ori}), \quad (1)$$

where $G(\cdot)$ and T_{gen} denote the image caption model and the generated caption, respectively.

3.2. Text-to-image generation module

We leverage the pre-trained text-to-image model to generate new images based on the image caption, transforming the caption from text modality to image modality. Specifically, the process of generating the image from the caption can be formulated as:

$$I_{gen} = F(T_{gen}) = F(G(I_{ori})), \quad (2)$$

where F denotes the text-to-image model. Our framework evaluates the generated image with the original image through the cyclic evaluation metric, eliminating the need for reference captions. Moreover, the cycle consistency in our approach is cross-modality, which transforms captions into images and compares them within the same image modality to mitigate the impact of the modality gap.

3.3. Cyclic evaluation metric

After we obtain the generated image based on the caption through the text-to-image model, we evaluate the generated image against the original image through the cyclic evaluation metric. Specifically, we elaborate a three-level evaluation framework $D(I_{ori}, I_{gen})$ in the following parts:

Pixel level. The pixel-level evaluation directly reflects the difference between difference between the generated image and the original image. In specific, we calculate the L_p norm (Minkowski Distance) between the original image I_{ori} and the generated image I_{gen} by pixel level, as shown

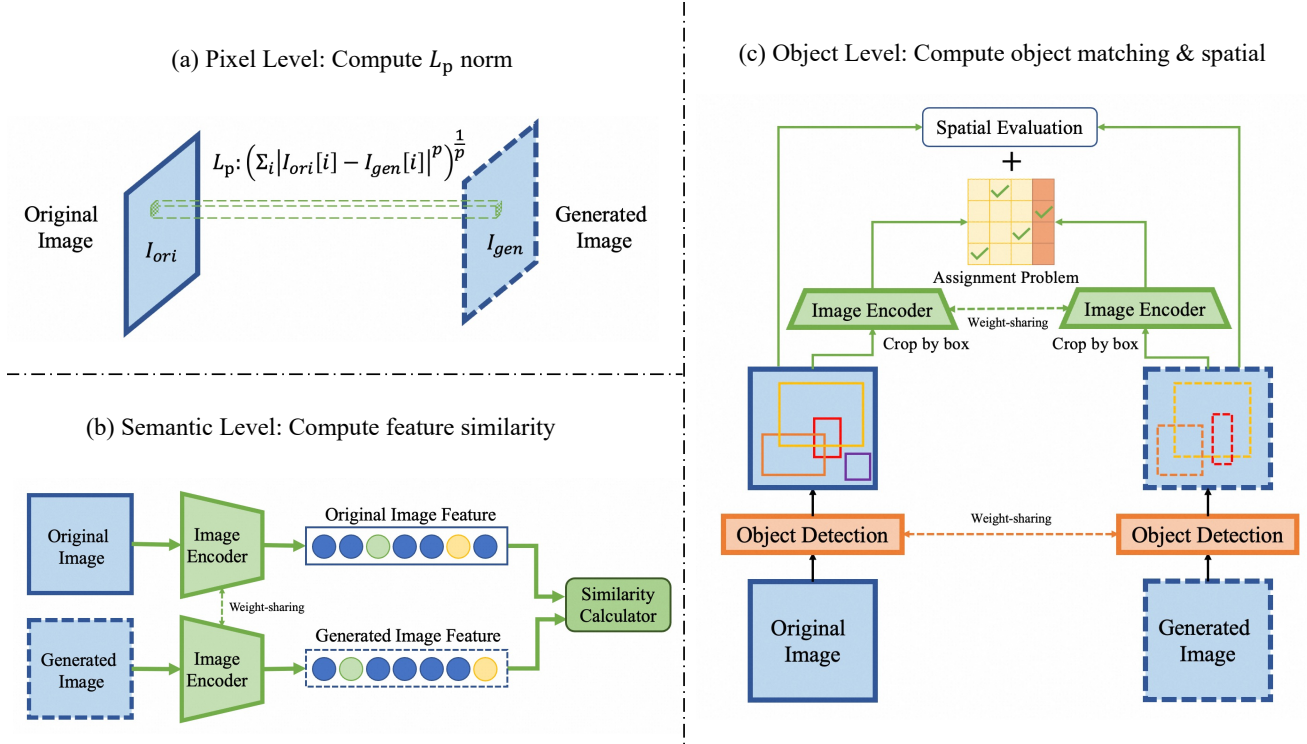


Figure 3. Illustration of our proposed evaluation metrics: (a) Calculate the pixel-by-pixel differences as pixel-level evaluation, (b) Calculate the similarity between the features of the original image and the generated image as semantic-level evaluation, (c) Detection-based object-level evaluation, taking into account both object matching and spatial relationship.

in (a) of Figure 3. The calculation process can be formulated as follows:

$$\mathcal{L}_{pix} = \left(\sum_i |I_{ori}[i] - I_{gen}[i]|^p \right)^{\frac{1}{p}}. \quad (3)$$

Equation (3) enables a quantitative assessment of the pixel-wise discrepancies between the original and generated images, thereby providing a fine-grained evaluation within CAMScore.

Semantic level. To assess the overall semantic information of an image, we perform semantic-level evaluation utilizing a pre-trained image encoder as the image feature extraction module. This encoder takes an image as input to generate a feature vector that represents the semantic content of the input image. We then calculate the similarity between the features of the original image and the generated image. Specifically, we employ a pre-trained ViT-B16 [32] as an exemplary model for image feature extraction. The ViT-B16 model is capable of generating rich and robust image representations, making it highly effective for various computer vision tasks. As for similarity calculation, we adopt

cosine similarity as the metric:

$$\mathcal{L}_{sem} = \frac{\langle \phi(I_{ori}), \phi(I_{gen}) \rangle}{\|\phi(I_{ori})\|_2 \cdot \|\phi(I_{gen})\|_2}, \quad (4)$$

where $\phi(\cdot)$ denotes the image feature extraction module, $\|\cdot\|_2$ denotes the Euclidean norm of vectors and $\langle \cdot, \cdot \rangle$ denotes the inner product of vectors. This approach enables a holistic comparison of the semantic content between images, thereby enhancing the evaluation robustness of CAMScore.

Object level. While semantic-level evaluation provides a holistic assessment of an entire image, it lacks the granularity required for detailed analysis. To achieve a more fine-grained evaluation, we introduce a detection-based object-level evaluation metric that yields detailed information. This approach involves applying an object detection model to both the original and generated images. For each detected object, the detection model outputs its corresponding bounding box. Utilizing these bounding boxes, we crop the objects and extract their feature representations f_{ori} from the original image and f_{gen} from the generated image using

the image feature extraction module $\phi(\cdot)$:

$$f_{ori} = \{\phi(B_{ori}^i(I_{ori}))\}_{i=1}^m, f_{gen} = \{\phi(B_{gen}^j(I_{gen}))\}_{j=1}^n, \quad (5)$$

where $\{B_{ori}^i\}_{i=1}^m$ and $\{B_{gen}^j\}_{j=1}^n$ denote the sets of m and n bounding boxes for the original images I_{ori} and generated images I_{gen} , respectively. Subsequently, we can compute the object-level similarity matrix between the original and generated images and derive the corresponding cost matrix:

$$S[i, j] = \frac{\langle f_{ori}[i], f_{gen}[j] \rangle}{\|f_{ori}[i]\|_2 \cdot \|f_{gen}[j]\|_2}, \quad (6)$$

$$\text{Cost}[i, j] = 1 - \frac{\langle f_{ori}[i], f_{gen}[j] \rangle}{\|f_{ori}[i]\|_2 \cdot \|f_{gen}[j]\|_2}. \quad (7)$$

To penalize discrepancies in object counts between the original and generated images, when $m > n$, we pad the cost matrix to an $m \times m$ matrix with elements set to 1 (the maximum cost), thereby imposing a numerical penalty for missing objects. We model the cost matrix as a classical assignment problem and employ the Hungarian (Kuhn-Munkres) algorithm [21, 30] to determine the optimal object matching and compute the minimum matching cost:

$$\begin{aligned} \mathcal{L}_{obj} &= \min_X \sum_i \sum_j \text{Cost}[i, j] X[i, j] \\ \text{s.t.} \quad &\sum_{i=1}^m X[i, j] = 1, \quad j = 1, 2, \dots, n, \\ &\sum_{j=1}^n X[i, j] = 1, \quad i = 1, 2, \dots, m, \\ &X[i, j] \in \{0, 1\}. \end{aligned} \quad (8)$$

However, the matching cost primarily captures the presence and semantic similarity of objects, while neglecting their spatial information. To address this limitation, we incorporate a 3D-spatial relationship evaluation for the matching object pairs. We leverage the object detection algorithms to obtain 2D positional information and utilize depth estimation to acquire depth information, thereby enabling 3D-spatial relationship evaluation between matched object pairs. Specifically, for each box $B : (x_1, y_1, x_2, y_2)$, we calculate its relative position by normalizing it with respect to the size of the image and subsequently compute the Complete-IoU (CIoU) loss [46]. CIoU loss takes into account the Intersection over Union (IoU), normalized central point distance, and the consistency of aspect ratio:

$$\mathcal{L}_{CIoU} = 1 - \text{IoU} + \frac{d^2}{c^2} + \alpha v, \quad (9)$$

where c is the diagonal length of the smallest enclosing box covering two boxes, and d is the distance of central points of two boxes, α is the trade-off parameter, v measures the

consistency of the aspect ratios between the predicted and ground truth boxes. Additionally, we incorporate the scale-invariant error [9] to further refine the spatial relationship evaluation:

$$\mathcal{L}_{dep} = \frac{1}{n} \sum_i d_i^2 - \frac{1}{n^2} \left(\sum_i d_i \right)^2, \quad (10)$$

where $d_i = \log(I_{gen}[I]) - \log(I_{ori}[I])$ is the difference between the prediction and ground truth at pixel i , and n denotes the total number of pixels. The scale-invariant loss function measures the error magnitude by focusing only on the relative depth of each value set without considering the scale difference between the ground truth and the prediction. This combination of metrics enables a more comprehensive assessment of both the geometric alignment and depth consistency between matched objects. Therefore, our evaluation framework achieves enhanced robustness by effectively capturing semantic and spatial nuances in object relations. Subsequently, following the approach of [37], we employ a multilayer perceptron (MLP) to integrate the scores and compute the final score:

$$\text{CAMScore} = \text{MLP}(\mathcal{L}_{pix}, \mathcal{L}_{sem}, \mathcal{L}_{obj}, \mathcal{L}_{CIoU}, \mathcal{L}_{dep}) \quad (11)$$

For the loss function, we adopted the Mean Squared Error (MSE), a conventional choice in regression tasks due to its proven efficacy in quantifying the discrepancy between predicted values and ground truth human judgments. Additional details can be found in the Appendix.

4. Experiments

4.1. Evaluation datasets

Human correlation and accuracy represent critical measures for evaluating image captioning metrics. To assess the caption-level correlation between automatic metrics and human judgments, we utilize the Flickr8k [14] and Composite dataset [1], wherein human annotators provide evaluations for each candidate caption. Following previous works [13, 24, 33], we compute Kendall's correlation coefficient τ_b and τ_c to measure the alignment between human judgments and metric scores. Kendall's correlation coefficient is a statistic used to measure the ordinal association between two measurements. For datasets of a different nature, like Pascal-50S [36], where annotators are tasked with selecting the superior caption from pairs of candidate captions, we assess performance using metric pairwise ranking accuracy.

Flickr8k-Expert. [14] Flickr8k-Expert dataset contains 17k expert annotations for image-caption pairs, encompassing a total of 5,664 distinct images. Each image-caption pair is evaluated by three expert annotators with scores

Metric	Flickr8k-Expert		Flickr8k-CF	
	Kendall τ_b	Kendall τ_c	Kendall τ_b	Kendall τ_c
BLEU-1 [31]	32.2	32.3	17.9	9.3
BLEU-4 [31]	30.6	30.8	16.9	8.7
ROUGE [27]	32.1	32.3	19.9	10.3
METEOR [6]	41.5	41.8	22.2	11.5
CIDEr [36]	43.6	43.9	24.6	12.7
SPICE [2]	51.7	44.9	24.4	12.0
BERT-S [44]	-	39.2	22.8	-
BERT-S++ [42]	-	46.7	-	-
TIGEr [18]	-	49.3	-	-
ViLBERTScore [23]	-	50.1	-	-
MID [20]	-	<u>54.9</u>	<u>37.3</u>	-
UMIC [24]	-	46.8	-	-
CLIP-S [13]	51.1	51.2	34.4	17.7
PAC-S [33]	<u>53.9</u>	54.3	36.0	<u>18.6</u>
CAMScore	54.8	55.6	37.5	19.3

Table 1. The Kendall correlation coefficient τ_b and τ_c between human judgments and various automatic metrics on Flickr8k-Expert and Flickr8k-CF [14] datasets. Bold font indicates the highest recorded value overall, while underlining indicates the second-highest value. The first part is for reference-based methods, and the second part is for reference-free methods.

Metric	Composite	
	Kendall τ_b	Kendall τ_c
BLEU-1 [31]	29.0	31.3
BLEU-4 [31]	28.3	30.6
ROUGE [27]	30.0	32.4
METEOR [6]	36.0	38.9
CIDEr [36]	34.9	37.7
SPICE [2]	38.8	40.3
BERT-S [44]	-	30.1
BERT-S++ [42]	-	44.9
TIGEr [18]	-	45.4
ViLBERTScore [23]	-	52.4
MID [20]	-	55.7
UMIC [24]	-	<u>56.1</u>
CLIP-S [13]	49.8	53.8
PAC-S [33]	<u>51.5</u>	55.7
CAMScore	53.4	57.5

Table 2. The Kendall correlation coefficient τ_b and τ_c between human judgments and various automatic metrics on the Composite dataset [1]. Bold font indicates the highest recorded value overall, while underlining indicates the second-highest value.

ranging from 1 (irrelevant) to 4 (perfect match).

Flickr8k-CF. [14] Flickr8k-CF consists of 145k binary quality judgments, collected from CrowdFlower, covering 48k image-caption pairs that contain 1k unique images. Each pair involves three annotators to determine whether the image-caption pair matches, categorized as either “yes” or “no”. The score for each pair is the proportion of “yes” responses.

Metric	HC	HI	HM	MM	Mean
BLEU-1 [31]	64.6	95.2	91.2	60.7	77.9
BLEU-4 [31]	60.3	93.1	85.7	57.0	74.0
ROUGE [27]	63.9	95.0	92.3	60.9	78.0
METEOR [6]	66.0	97.7	94.0	66.6	81.1
CIDEr [36]	66.5	97.9	90.7	65.2	80.1
SPICE [2]	63.6	96.3	86.7	68.3	78.7
BERT-S [44]	65.4	96.2	93.3	61.4	79.1
BERT-S++ [42]	65.4	98.1	96.4	60.3	80.1
TIGEr [18]	56.0	99.8	92.8	74.2	80.7
ViLBERTScore [23]	49.9	99.6	93.1	75.8	79.6
MID [20]	67.0	<u>99.7</u>	<u>97.4</u>	76.8	<u>85.2</u>
UMIC [24]	66.1	99.8	98.1	76.2	85.1
CLIP-S [13]	55.9	99.3	96.5	72.0	80.9
PAC-S [33]	60.6	99.3	96.9	72.9	82.4
CAMScore	68.8	99.6	<u>97.4</u>	77.4	85.8

Table 3. Caption pairwise ranking accuracy results on the Pascal-50S dataset [36], obtained by averaging the scores over five random draws of reference captions (except for reference-free metrics). Bold font indicates the highest recorded value overall, while underlining indicates the second-highest value.

Composite. [1] Composite dataset comprises human judgments of 12,000 image-caption pairs, incorporating 3,995 images from MSCOCO (2,007 images) [28], Flickr30K (991 images) [43], and Flickr8k (997 images) [14]. Human evaluators were asked to rate each image-caption pair and assign a score on a scale of 1 to 5 to estimate how well the caption is aligned with the associated image.

Pascal-50S. [36] Pascal-50S includes 4,000 caption pairs associated with 1,000 images, along with a label indicating which of the two captions is deemed correct by 48 annotators. Each image is linked to approximately 50 reference captions. In Pascal-50S, caption pairs are categorized based on the composition of the two captions: HC denotes two correct human-written captions; HI indicates one correct and one incorrect human-written caption; HM represents one human-written caption and one machine-generated caption; and MM denotes two machine-generated captions.

4.2. Baselines

All baseline metrics have been briefly introduced in Section 2. Specifically, we adopt BLEU [31], ROUGE [27], METEOR [6], CIDEr [36], SPICE [2], BERTSCORE [44], TIGEr [18], ViLBERTScore [23], and MID [20] as baseline metrics due to their reliance on references for evaluating image captioning tasks. Additionally, we incorporate UMIC [24], CLIPScore [13], and PAC-S [33] as baseline metrics because they are reference-free evaluation metrics for image captioning.

Metric	Flickr8k-Expert [14]		Flickr8k-CF [14]		Composite [1]		Pascal-50S [36]				
	Kendall τ_b	Kendall τ_c	Kendall τ_b	Kendall τ_c	Kendall τ_b	Kendall τ_c	HC	HI	HM	MM	Mean
w/o pixel	53.9 (-0.9)	54.1 (-1.5)	35.6 (-1.9)	18.3 (-1.0)	51.2 (-2.2)	55.4 (-2.1)	67.5	98.9	96.3	76.1	84.7 (-1.1)
w/o semantic	43.2 (-11.6)	43.5 (-12.1)	24.7 (-12.8)	12.3 (-7.0)	35.1 (-18.3)	33.5 (-24.0)	63.4	94.5	89.1	65.8	78.2 (-7.6)
w/o object	51.3 (-3.5)	51.4 (-4.2)	34.1 (-3.4)	16.9 (-2.4)	50.2 (-3.2)	54.1 (-3.4)	65.2	96.8	94.9	73.8	82.7 (-3.1)
w/o box	53.1 (-1.7)	53.6 (-2.0)	35.2 (-2.3)	17.7 (-1.6)	50.7 (-2.7)	54.6 (-2.9)	65.8	97.1	95.2	75.3	83.4 (-2.4)
w/o depth	53.4 (-1.4)	53.7 (-1.9)	35.4 (-2.1)	18.0 (-1.3)	50.9 (-2.5)	54.9 (-2.6)	66.7	98.2	95.5	75.7	84.0 (-1.8)

Table 4. Ablation study results in which scores from each evaluation level are excluded. The numbers in brackets indicate how much the method has decreased relative to the baseline. These results are assessed using Kendall’s correlation coefficients τ_b and τ_c on the Flickr8k-Expert, Flickr8k-CF [14], and Composite datasets [1], along with pairwise ranking accuracy on the Pascal-50S dataset [36].

4.3. Implementation details

In our framework, we utilize FLUX.1 [dev] [22] as the text-to-image model. For the measurement of pixel level, we adopt the Euclidean distance metric, corresponding to $p = 2$ in Equation (3). This choice effectively quantifies the spatial discrepancies between corresponding pixel values. For the image feature extraction module, we employ the pre-trained ViT-B16 architecture, utilizing the image encoder component from CLIP [32]. For the object level, we utilize YOLOv8 [19] as the object detector due to its stable and excellent performance and efficiency in object detection tasks. Besides, we integrate Depth Anything V2 [41] to incorporate depth estimation capabilities, thereby enhancing the model’s ability to analyze the 3D-spatial relationship within the scene. This combination of advanced object detection and depth estimation frameworks facilitates a more comprehensive analysis, ensuring robust performance across diverse application scenarios. Additional implementation details can be found in the Appendix.

4.4. Correlation with human judgment

We first evaluate our CAMScore on the Flickr8k-Expert and Flickr8k-CF [14] datasets. Consistent with previous works, we compute the Kendall correlation coefficient τ_b and τ_c . The results, as shown in Table 1, compare CAMScore’s performance against the baseline metrics mentioned in Section 4.2. The first part of the table is for reference-based methods, and the second part is for reference-free methods. The experimental results demonstrate that CAMScore exhibits a strong correlation with human judgments across considered datasets, thereby affirming its superiority over previously proposed metrics. In particular, CAMScore improves the Kendall correlation coefficient τ_b and τ_c by 0.9 and 1.3 points compared to PAC-S on the Flickr8k-Expert dataset, and by 1.5 and 0.7 points compared to PAC-S on the Flickr8k-CF dataset, respectively. Notably, CAMScore significantly outperforms the correlation coefficient achieved by evaluation metrics that necessitate reference captions, highlighting its superior ability to align with human judgments without dependence on reference annotations.

We further conducted experiments on the Composite

dataset [1]. The experiment results, shown in Table 2, are also presented in terms of Kendall τ_b and Kendall τ_c correlation coefficient. CAMScore achieves the best correlation with human judgment among all baseline metrics, improving by 1.9 on the τ_b correlation coefficient and 1.8 on the τ_c correlation coefficient over the second highest score. These improvements demonstrate the comprehensive effectiveness of CAMScore in aligning with human judgments across diverse benchmarking scenarios.

4.5. Accuracy on pairwise ranking

We assess the effectiveness of CAMScore on the Pascal-50S dataset [36], which provides pairwise preference judgments between two captions. The caption that received the majority vote was deemed the preferred choice. In this setting, instead of computing Kendall correlation scores, we compute pairwise accuracy by considering for each pair the caption preferred by the majority of human ratings as correct and measuring how often the evaluation metric assigns a higher score to the selected caption. Section 4.2 presents the accuracy results for Pascal-50S. In our experiments, CAMScore achieves state-of-the-art (SOTA) results with a mean accuracy of 85.8, proving the general effectiveness of our approach. Besides, CAMScore achieves state-of-the-art (SOTA) results with accuracies of 68.8 and 77.4 for HC and MM respectively. Although CAMScore does not attain the highest accuracy for the HI and HM, its performance remains closely comparable to existing SOTA accuracy. These results provide strong evidence that our metric is on par with the strong baselines and can therefore serve as a potent automatic evaluation metric for image captioning.

4.6. Ablation study

We investigate the impact of various score integration strategies on overall performance. Specifically, we remove the scores of integration respectively to verify the impact of each score on the performance, as shown in Table 4. The performance without the semantic level metric is the lowest across all benchmark datasets, indicating that the semantic level poses an important role in the proposed metric. In addition, the impact of object level is the second largest,



Figure 4. Examples of successful (a,b,c) and failed (d) cases. Except for the last non-photorealistic case, all others are from the Flickr8K dataset. The first column is the original image and the last three columns are the generated images with captions and metrics. Human judgment prefers the leftmost caption and dislikes the rightmost caption. Our metric is more consistent with human judgment.

which illustrates the effectiveness of our design for object matching and quantity penalties. The absence of pixel level has the least impact on the performance, indicating that direct pixel differences are less relevant to human judgment. By systematically evaluating the influence of each evaluated score, we verified that metrics at each level are necessary.

4.7. Case study

Figure 4 shows various example of CAMScore. For each case, we provide three different captions along with their corresponding scores. All methods are capable of distinguishing irrelevant captions for photo-style images, as illustrated in the last column. However, performance diminishes when other metrics deal with more detailed problems. Specifically, CLIPScore confuses the positional relationship and corresponding numeracy of man and dogs, and confuses the scenes where the child is for the first two columns of Figure 4 (a) and (c), respectively. PAS-S confuses the numeracy of dogs for the first two columns of Figure 4 (b). In

contrast, CAMScore accurately captures attribute and location information, aligning closely with human judgment.

4.8. Limitations and future works

CAMScore is constrained by the detection performance of the object detector employed in the framework. Current SOTA object detection models are primarily based on the MS-COCO dataset, which has a limited number of specific categories. Besides, object detectors generally exhibit sub-optimal performance for non-photorealistic images, leading to failure of CAMScore, as shown in the last row in Figure 4. These limitations may be eliminated with the future development of more powerful object detectors. In addition, text-to-image models usually require longer processing times and more computational resources compared to object detection models. In future work, we aim to incorporate the metric into model training procedures to enhance specific capabilities.

5. Conclusion

In this paper, we proposed CAMScore, a novel cyclic reference-free evaluation metric for image captioning. CAMScore enables reference-free evaluation while addressing the modality gap inherent in existing cross-modality metrics by leveraging the cycle consistency between image captioning and text-to-image generation. Additionally, our three-level modular framework provides fine-grained information for evaluation from the pixel-level, semantic-level, and object-level. Furthermore, experimental comparisons with baseline metrics across various benchmarks demonstrate that CAMScore has a strong correlation with human judgment, showing the effectiveness of the proposed metric.

References

- [1] Somak Aditya, Yezhou Yang, Chitta Baral, Cornelia Fermuller, and Yiannis Aloimonos. From Images to Sentences through Scene Description Graphs using Commonsense Reasoning and Knowledge. *arXiv preprint arXiv:1511.03292*, 2015. 2, 5, 6, 7, 1
- [2] Peter Anderson, Basura Fernando, Mark Johnson, and Stephen Gould. SPICE: Semantic propositional image caption evaluation. In *ECCV*, pages 382–398, 2016. 2, 6
- [3] Peter Anderson, Xiaodong He, Chris Buehler, Damien Teney, Mark Johnson, Stephen Gould, and Lei Zhang. Bottom-Up and Top-Down Attention for Image Captioning and Visual Question Answering. In *CVPR*, pages 6077–6086, 2018. 1
- [4] Jinbin Bai, Chunhui Liu, Feiyue Ni, Haofan Wang, Mengying Hu, Xiaofeng Guo, and Lele Cheng. LaT: Latent Translation with Cycle-Consistency for Video-Text Retrieval. *arXiv preprint arXiv:2207.04858*, 2022. 3
- [5] Jinbin Bai, Tian Ye, Wei Chow, Enxin Song, Qing-Guo Chen, Xiangtai Li, Zhen Dong, Lei Zhu, and Shuicheng Yan. Meissonic: Revitalizing Masked Generative Transformers for Efficient High-Resolution Text-to-Image Synthesis. *arXiv preprint arXiv:2410.08261*, 2024. 1
- [6] Satanjeev Banerjee and Alon Lavie. METEOR: An Automatic Metric for MT Evaluation with Improved Correlation with Human Judgments. In *Proceedings of the ACL Workshop on Intrinsic and Extrinsic Evaluation Measures for Machine Translation and/or Summarization*, pages 65–72. Association for Computational Linguistics, 2005. 2, 6
- [7] Yen-Chun Chen, Linjie Li, Licheng Yu, Ahmed El Kholy, Faisal Ahmed, Zhe Gan, Yu Cheng, and Jingjing Liu. UNITER: UNiversal Image-TEXT Representation Learning. In *ECCV*, pages 104–120, 2020. 3
- [8] Jacob Devlin, Ming-Wei Chang, Kenton Lee, and Kristina Toutanova. BERT: Pre-training of Deep Bidirectional Transformers for Language Understanding. In *Proceedings of the 2019 Conference of the North American Chapter of the Association for Computational Linguistics: Human Language Technologies, Volume 1 (Long and Short Papers)*, pages 4171–4186, 2019. 2
- [9] David Eigen, Christian Puhersch, and Rob Fergus. Depth Map Prediction from a Single Image using a Multi-Scale Deep Network. In *NeurIPS*, pages 2366–2374, 2014. 5
- [10] Clément Godard, Oisín Mac Aodha, and Gabriel J Brostow. Unsupervised Monocular Depth Estimation with Left-Right Consistency. In *CVPR*, pages 270–279, 2017. 3
- [11] Longteng Guo, Jing Liu, Peng Yao, Jiangwei Li, and Hanqing Lu. MSCap: Multi-Style Image Captioning with Unpaired Stylized Text. In *CVPR*, pages 4204–4213, 2019. 3
- [12] Danna Gurari, Yinan Zhao, Meng Zhang, and Nilavra Bhattacharya. Captioning Images Taken by People Who Are Blind. In *ECCV*, pages 417–434. Springer, 2020. 1
- [13] Jack Hessel, Ari Holtzman, Maxwell Forbes, Ronan Le Bras, and Yejin Choi. CLIPScore: A Reference-free Evaluation Metric for Image Captioning. In *Proceedings of the 2021 Conference on Empirical Methods in Natural Language Processing*, pages 7514–7528. Association for Computational Linguistics, 2021. 1, 2, 3, 5, 6
- [14] Micah Hodosh, Peter Young, and Julia Hockenmaier. Framing image description as a ranking task: Data, models and evaluation metrics. *Journal of Artificial Intelligence Research*, 47:853–899, 2013. 2, 5, 6, 7, 1
- [15] Judy Hoffman, Eric Tzeng, Taesung Park, Jun-Yan Zhu, Phillip Isola, Kate Saenko, Alexei Efros, and Trevor Darrell. CyCADA: Cycle-Consistent Adversarial Domain Adaptation. In *ICML*, pages 1989–1998. Pmlr, 2018. 3
- [16] Anwen Hu, Shizhe Chen, and Qin Jin. Question-controlled Text-aware Image Captioning. In *ACM MM*, pages 3097–3105, 2021. 1
- [17] Anwen Hu, Shizhe Chen, Liang Zhang, and Qin Jin. InfoMetIC: An informative metric for reference-free image caption evaluation. In *Proceedings of the 61st Annual Meeting of the Association for Computational Linguistics (Volume 1: Long Papers)*, pages 3171–3185. Association for Computational Linguistics, 2023. 3
- [18] Ming Jiang, Qiuyuan Huang, Lei Zhang, Xin Wang, Pengchuan Zhang, Zhe Gan, Jana Diesner, and Jianfeng Gao. TIGER: Text-to-Image Grounding for Image Caption Evaluation. In *Proceedings of the 2019 Conference on Empirical Methods in Natural Language Processing and the 9th International Joint Conference on Natural Language Processing (EMNLP-IJCNLP)*, pages 2141–2152. Association for Computational Linguistics, 2019. 1, 2, 6
- [19] Glenn Jocher, Ayush Chaurasia, and Jing Qiu. Ultralytics YOLOv8, 2023. 7
- [20] Jin-Hwa Kim, Yunji Kim, Jiyoung Lee, Kang Min Yoo, and Sang-Woo Lee. Mutual Information Divergence: A Unified Metric for Multimodal Generative Models. In *NeurIPS*, pages 35072–35086, 2022. 2, 6
- [21] Harold W Kuhn. The Hungarian Method for the Assignment Problem. *Naval research logistics quarterly*, 2(1-2):83–97, 1955. 5
- [22] Black Forest Labs. FLUX.1 [dev], 2024. 7, 1
- [23] Hwanhee Lee, Seunghyun Yoon, Franck Dernoncourt, Doo Soon Kim, Trung Bui, and Kyomin Jung. ViLBERTScore: Evaluating image caption using vision-and-language BERT. In *Proceedings of the First Workshop on Evaluation and Comparison of NLP Systems*, pages 34–39. Association for Computational Linguistics, 2020. 1, 2, 6
- [24] Hwanhee Lee, Seunghyun Yoon, Franck Dernoncourt, Trung Bui, and Kyomin Jung. UMIC: An Unreferenced Metric for Image Captioning via Contrastive Learning. In *Proceedings of the 59th Annual Meeting of the Association for Computational Linguistics and the 11th International Joint Conference on Natural Language Processing (Volume 2: Short Papers)*, pages 220–226, 2021. 1, 2, 3, 5, 6
- [25] Yebin Lee, Imseong Park, and Myungjoo Kang. FLEUR: An Explainable Reference-Free Evaluation Metric for Image Captioning Using a Large Multimodal Model. In *Proceedings of the 62nd Annual Meeting of the Association for Computational Linguistics (Volume 1: Long Papers)*, pages 3732–3746. Association for Computational Linguistics, 2024. 3

- [26] Victor Weixin Liang, Yuhui Zhang, Yongchan Kwon, Serena Yeung, and James Y Zou. Mind the Gap: Understanding the Modality Gap in Multi-modal Contrastive Representation Learning. In *NeurIPS*, pages 17612–17625, 2022. 2
- [27] Chin-Yew Lin. ROUGE: A package for automatic evaluation of summaries. In *Text summarization branches out*, pages 74–81, 2004. 2, 6
- [28] Tsung-Yi Lin, Michael Maire, Serge Belongie, James Hays, Pietro Perona, Deva Ramanan, Piotr Dollár, and C Lawrence Zitnick. Microsoft COCO: Common Objects in Context. In *ECCV*, pages 740–755. Springer, 2014. 6, 1
- [29] Jiasen Lu, Dhruv Batra, Devi Parikh, and Stefan Lee. ViLBERT: Pretraining Task-Agnostic Visiolinguistic Representations for Vision-and-Language Tasks. In *NeurIPS*, pages 13–23, 2019. 2
- [30] James Munkres. Algorithms for the Assignment and Transportation Problems. *Journal of the society for industrial and applied mathematics*, 5(1):32–38, 1957. 5
- [31] Kishore Papineni, Salim Roukos, Todd Ward, and Wei-Jing Zhu. BLEU: a method for automatic evaluation of machine translation. In *Proceedings of the 40th annual meeting of the Association for Computational Linguistics*, pages 311–318, 2002. 2, 6
- [32] Alec Radford, Jong Wook Kim, Chris Hallacy, Aditya Ramesh, Gabriel Goh, Sandhini Agarwal, Girish Sastry, Amanda Askell, Pamela Mishkin, Jack Clark, et al. Learning Transferable Visual Models From Natural Language Supervision. In *International conference on machine learning*, pages 8748–8763. PMLR, 2021. 3, 4, 7, 1
- [33] Sara Sarto, Manuele Barraco, Marcella Cornia, Lorenzo Baraldi, and Rita Cucchiara. Positive-Augmented Contrastive Learning for Image and Video Captioning Evaluation. In *CVPR*, pages 6914–6924, 2023. 3, 5, 6
- [34] Meet Shah, Xinlei Chen, Marcus Rohrbach, and Devi Parikh. Cycle-Consistency for Robust Visual Question Answering. In *CVPR*, pages 6649–6658, 2019. 3
- [35] Peiyang Shi, Michael C. Welle, Márten Björkman, and Danica Kragic. Towards understanding the modality gap in CLIP. In *ICLR 2023 Workshop on Multimodal Representation Learning: Perks and Pitfalls*, 2023. 2
- [36] Ramakrishna Vedantam, C Lawrence Zitnick, and Devi Parikh. CIDEr: Consensus-based image description evaluation. In *CVPR*, pages 4566–4575, 2015. 2, 5, 6, 7, 1
- [37] Yuiga Wada, Kanta Kaneda, Daichi Saito, and Komei Suguiura. Polos: Multimodal Metric Learning from Human Feedback for Image Captioning. In *CVPR*, pages 13559–13568, 2024. 5
- [38] Ning Wang, Yibing Song, Chao Ma, Wengang Zhou, Wei Liu, and Houqiang Li. Unsupervised Deep Tracking. In *CVPR*, pages 1308–1317, 2019. 3
- [39] Sijin Wang, Ziwei Yao, Ruiping Wang, Zhongqin Wu, and Xilin Chen. FAIEr: Fidelity and Adequacy Ensured Image Caption Evaluation. In *CVPR*, pages 14050–14059, 2021. 1, 2
- [40] Kelvin Xu, Jimmy Ba, Ryan Kiros, Kyunghyun Cho, Aaron Courville, Ruslan Salakhudinov, Rich Zemel, and Yoshua Bengio. Show, attend and tell: Neural image caption generation with visual attention. In *ICML*, pages 2048–2057. PMLR, 2015. 1
- [41] Lihe Yang, Bingyi Kang, Zilong Huang, Zhen Zhao, Xiaogang Xu, Jiashi Feng, and Hengshuang Zhao. Depth Anything V2. *arXiv preprint arXiv:2406.09414*, 2024. 7
- [42] Yanzhi Yi, Hangyu Deng, and Jinglu Hu. Improving Image Captioning Evaluation by Considering Inter References Variance. In *Proceedings of the 58th Annual Meeting of the Association for Computational Linguistics*, pages 985–994, 2020. 2, 6
- [43] Peter Young, Alice Lai, Micah Hodosh, and Julia Hockenmaier. From image descriptions to visual denotations: New similarity metrics for semantic inference over event descriptions. *Transactions of the Association for Computational Linguistics*, 2:67–78, 2014. 6, 1
- [44] Tianyi Zhang, Varsha Kishore, Felix Wu, Kilian Q Weinberger, and Yoav Artzi. BERTScore: Evaluating Text Generation with BERT. In *ICLR*, 2019. 2, 6
- [45] Wei Zhao, Maxime Peyrard, Fei Liu, Yang Gao, Christian M. Meyer, and Steffen Eger. MoverScore: Text Generation Evaluating with Contextualized Embeddings and Earth Mover Distance. In *Proceedings of the 2019 Conference on Empirical Methods in Natural Language Processing and the 9th International Joint Conference on Natural Language Processing (EMNLP-IJCNLP)*, pages 563–578. Association for Computational Linguistics, 2019. 2
- [46] Zhaohui Zheng, Ping Wang, Dongwei Ren, Wei Liu, Rongguang Ye, Qinghua Hu, and Wangmeng Zuo. Enhancing Geometric Factors in Model Learning and Inference for Object Detection and Instance Segmentation. *IEEE transactions on cybernetics*, 52(8):8574–8586, 2021. 5
- [47] Jun-Yan Zhu, Taesung Park, Phillip Isola, and Alexei A. Efros. Unpaired Image-to-Image Translation Using Cycle-Consistent Adversarial Networks. In *ICCV*, pages 2242–2251, 2017. 3

Evaluating Image Caption via Cycle-consistent Text-to-Image Generation

Supplementary Material

6. Implementation details

6.1. Dataset Setup

Flickr8k-Expert. [14] Flickr8k-Expert dataset contains 17k expert annotations for image-caption pairs, encompassing a total of 5,664 distinct images. The captions in Flickr 8K were selected by an image retrieval system from a reference caption pool, instead of generated using a learned image captioning model. Each image-caption pair is evaluated by three expert annotators with scores ranging from 1 to 4, where a score of 1 indicates that the caption does not correlate with the image and a score of 4 signifies that the caption describes the corresponding image without errors. This evaluation methodology ensures a reliable assessment of caption quality in relation to the visual content.

Flickr8k-CF. [14] Flickr8k-CF consists of 145k binary quality judgments, collected from CrowdFlower, covering 48k image-caption pairs that contain 1k unique images. For each pair, three annotators determine whether the image-caption pair is a valid match, categorizing their responses as either “yes” or “no”. The final score for each image-caption pair is calculated as the proportion of “yes” responses.

Composite. [1] Composite dataset comprises human judgments of 12,000 image-caption pairs, incorporating 3,995 images from MSCOCO (2,007 images) [28], Flickr30K (991 images) [43], and Flickr8k (997 images) [14]. Candidate captions were sourced from both human reference captions and two captioning models. In this dataset, human evaluators score each caption’s relevance to its corresponding image using a five-point scale, where 1 indicates that “the description has nothing to do with the image” and 5 signifies that “the description is perfectly relevant to the image.”

Pascal-50S. [36] Pascal-50S includes 4,000 caption pairs associated with 1,000 images from UIUC PASCAL Sentence Dataset. Each pair is annotated to indicate which of the two captions is considered correct by 48 annotators. Each image is linked to approximately 50 reference captions generated by humans. Annotators are tasked with selecting the candidate caption in each pair that most closely aligns with the provided reference descriptions. In Pascal-50S, caption pairs are categorized based on the composition of the two captions: 1) Human-Human Correct (HC) contains two human-written captions for the target im-

age, 2) Human-Human Incorrect (HI) includes two captions written by humans but describing different images, 3) the group of Human-Machine (HM) contains a human written and a machine-generated caption, and 4) Machine-Machine (MM) includes two matching generated captions focusing on the same image.

6.2. Experiment details

In our framework, we utilize FLUX.1 [dev] [22] as the text-to-image model. For the measurement of pixel level, we adopt the Euclidean distance metric, corresponding to $p = 2$. This choice effectively quantifies the spatial discrepancies between corresponding pixel values. For the image feature extraction module, we employ the pre-trained ViT-B16 architecture, utilizing the image encoder component from CLIP [32]. In the ViT-B16 architecture, the input image is divided into patches, which are then transformed into vectors through embedding layers. These vectors are subsequently processed by Transformer blocks that consist of self-attention and feed-forward layers. For the object level, we utilize YOLOv8x, the largest model in the YOLOv8 family as the object detector due to its stable and excellent performance and efficiency in object detection tasks. Besides, we integrate Depth Anything v2-Large, which is also the largest model currently available in the Depth Anything v2 family to incorporate depth estimation capabilities, thereby enhancing the model’s ability to analyze the 3D-spatial relationship within the scene. This combination of advanced object detection and depth estimation frameworks facilitates a more comprehensive analysis, ensuring robust performance across diverse application scenarios. When evaluating the original image with the generated image, we resize the original image to 512×512 for ease of calculation. The inputs are first transformed by the sigmoid function and then passed to the multilayer perceptron. We use a batch size of 64, a learning rate of $3e-5$, and used early stopping in our model to optimize for the highest Kendall’s τ . We implement CAMScore with PyTorch and train on a NVIDIA A100 GPU. We calculate the Kendall tau score using the SciPy 1.14.1 implementation.

7. Additional Results on case study

We provide the results of object detection and depth estimation for each case in the case study. As shown in Figure 5, the object detector successfully boxes the objects in case (a,b,c), while failing in the non-photorealistic case (d), and the failure of object detectors will affect our metric. The depth estimation performs well on objects across all

cases, indicating that the depth estimation method to estimate the depth of image objects is robust. Since our object level evaluation mainly relies on object-matching relations, the performance of object detectors will affect our metric. The failure of the object detector on the non-photorealistic image Figure 5 (d) is the reason why this case fails, indicating that the current object detector has a lot of room for improvement.

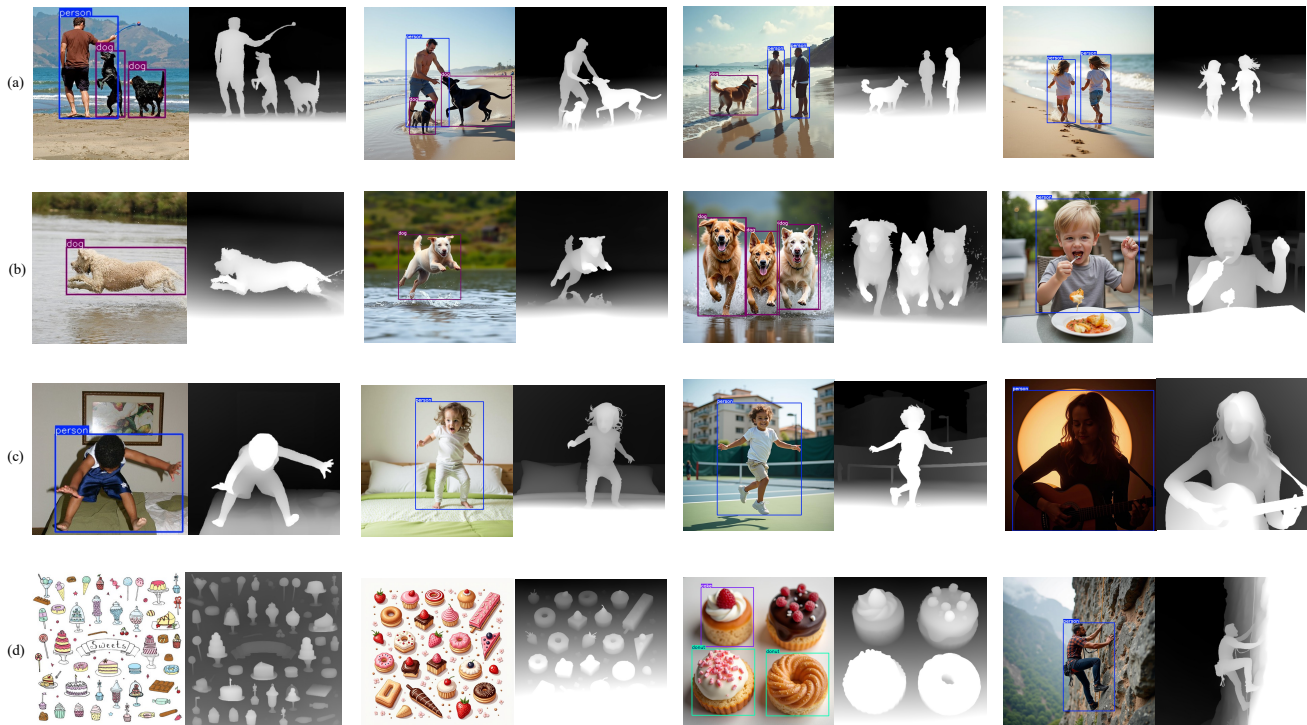


Figure 5. Object detection and depth estimation result of case study. The object detector successfully boxes the object in case (a,b,c), while failing in the non-photorealistic case (d).